



Robust Region Duplication Detection on Log-Polar Domain Using Band Limitation

Yue Yuan^{1,2} · Yun Zhang³ · Shuang Chen⁴ · Hong Wang⁵

Received: 5 February 2016 / Accepted: 27 June 2016 / Published online: 16 July 2016
© King Fahd University of Petroleum & Minerals 2016

Abstract Region duplication is one of the image-tampering techniques in which a part of image is copied and pasted into another region of the same image. In this paper, a robust duplication detection algorithm is proposed against severe degradations such as illumination changes, blurring, large scaling, noise contamination and JPEG compression. We introduce an adaptive phase correlation scheme in the log-polar domain, which is effective to locate the most salient local feature of an image patch on frequency band. By using the information collected from the band limitation, duplicated regions can be correctly located. Our contribution is to present a robust image duplication detection algorithm which can handle large scaling manipulation while pre-

serving detection performance under other manipulations or degradations. We perform degradation and comparison test on various tampered images, and experimental results show that the proposed algorithm achieves satisfactory performance.

Keywords Duplication detection · Log-polar domain · Band limitation · Scaling manipulation

Yun Zhang is the joint first author.

✉ Hong Wang
hongwang@mail.neu.edu.cn

Yue Yuan
yuanyuande2005@163.com

Yun Zhang
zhangyun_zju@zju.edu.cn

Shuang Chen
chenshuang19891129@gmail.com

¹ School of SINO-DUTCH Biomedical and Information Engineering, Northeastern University, Shenyang 110819, China

² School of Information Engineering, Shenyang University, Shenyang 110042, China

³ Institute of Zhejiang Radio and TV Technology, Zhejiang University of Media and Communications, Hangzhou 310018, China

⁴ School of Information Science and Engineering, Shenyang University of Technology, Shenyang 110870, China

⁵ School of Mechanical Engineering and Automation, Northeastern University, Shenyang 110819, China

1 Introduction

With the rapid development of multimedia and Internet technology, we have an ever-increasing availability of digital media, such as images and videos. However, maliciously tampered images are spreading rampantly due to the wide use of image editing softwares such as Photoshop, Picasa. Among the ways of image duplication, copy-move forgery is the most popular and common one, in which one part of an image is copied and pasted into another region of the same image to make up a scene or to conceal some information.

Region duplication detection, which is also called copy-move detection, has become a research focus in recent years. Fridrich et al. [1] proposed a block-matching algorithm which takes the quantified coefficients of discrete cosine transform of 8×8 patches as feature vectors and locates matching pairs among lexicographically sorted features. Popescu et al. [2] improved the aforementioned algorithm by introducing PCA to reduce the length of feature vector to 32; however, this algorithm cannot detect forgery with rotation. Similar algorithms are proposed by Li et al. [3] and Gul et al. [4], where SVD is adopted instead of PCA. Mahdian et al. [5] employed invariant blur moment to represent the feature in the patch.



While the above algorithms can only handle manipulations like translation or grayscale changes, some other algorithms are further proposed to detect geometric manipulations such as rotation, scaling or flipping. Bayram et al. [6] introduced FMT(Fourier–Mellin transform) to compare image patches which are invariant to scaling and rotation. Although this algorithm is robust to JPEG compression, in practice, it can only detect slight rotation and scaling because of the intrinsic geometric limitation of rectangular patch. Pan et al. [7] employed the SIFT feature to detect forgery, achieving good performance on detecting regions with large scaling, but this algorithm needs over 50 feature points in each patch. In the same year, Ryu et al. [8] proposed a copy-move forgery detection algorithm based on the Zernike moment which is a rotation invariant feature. Bravo-Solorio et al. [9] proposed a algorithm by projecting feature in a patch onto a 1D descriptor using log-polar coordinates. Shao et al. [10] proposed a phase correlation method based on polar expansion and adaptive band limitation for region duplication forgery detection. Owing to the circular window expansion and phase correlation, their method is effective for many difficult cases, such as copy-move, rotation, grayscale change. Though achieving promising performance, their method is not efficient due to the point-by-point scanning in circular windows matching. Wang et al. [11] proposed a new method for duplicated regions detection and localization by merging blur and affine moment invariants, which is also effective under some simple affine transforms and blur degradations. Chen et al. [12] proposed a novel region duplication detection method that is robust to general geometrical transformations. Kuo et al. [13] applied the dual spare features and structure similarity to enhance the detection performance of the region duplication. Zheng et al. [14] extracted Harris corner points and get binary descriptors of each key point, then located the tampered regions by comparing the similarity between descriptors. Tan et al. [15] presented a new framework for object recognition via weakly supervised metric and template learning.

Motivated by [10], which takes into account the local fractal dimension, we propose a robust image forgery detection approach. With the improved adaptive band limitation, our method can locate intrinsic feature and band of image patch in the frequency domain and detect duplicated regions robustly.

Our Main Contribution We extend the band limitation to the frequency domain of the log-polar coordinates of the image, in which an improved adaptive band limitation procedure is implemented to automatically select useful band for detection. With this scheme, forgery of large scaling (scaling ranging from 30–600 %) can be effectively detected using our algorithm.

This paper is organized as follows. In Sect. 1, a brief introduction and review of previous work is presented. In Sect. 2, the details of the proposed algorithm are elaborated. We give a comprehensive understanding on how the adaptive band

limitation works on log-polar domain. In Sect. 3, we tested our algorithm on massive test images with various types of manipulations and their mixture. Comparisons are further made to show advantages and disadvantages of the proposed algorithm. Finally, we conclude our work and give an analysis in Sect. 4.

2 Methodology

2.1 Patch Expression in Log-Polar Coordinates

First, color images are transformed into grayscale so that a log-polar expansion and Fourier transform can be applied. For a scanning patch in a color image, we expand the patch from Cartesian coordinates to log-polar coordinates using bilinear interpolation. This procedure ensures that the Fourier transform and band limitation framework can be utilized in log-polar coordinates where a point is identified by two numbers: logarithm of distance to center point and the rotation angle.

When a patch is expanded using log-polar coordinates, both scaling and rotation in original patch are performed in the new domain, which makes it possible to identify similar patches by the translation invariant features. The bilinear interpolation may introduce some instability or contamination in high-frequency band. Fortunately, the band limitation procedure can ensure the robustness of detection, which will be analyzed in Sects. 2.3 and 3.

The image patch size is essential to the detection performance. For practical use, we choose the size of overlapping patches to be 32×32 in experiments.

Assuming that height and width of each patch are the same, we define the log-polar expression of each patch as follows. For an image patch $I(p, q)$ ($p, q \in 1, \dots, 32$), the corresponding log-polar expression of patch is as follows.

$$\begin{cases} x = \log(\sqrt{p^2 + q^2}) \\ y = \arctan(p/q) \end{cases} \quad (1)$$

For computational efficiency in FFT(fast Fourier transform), the ranges containing grid of x and y as integer should be in the form 2^k , which is also the size of the expanded and interpolated image patches. In this work, we test different combinations of ranges along x and y , and set ranges of x and y to be 32 and 64 for the trade-off on computational complexity and performance. Figure 1 shows that an image is transformed into log-polar coordinates.

2.2 Phase Correlation to Detect Forgery

Phase correlation is a nonlinear algorithm based on the Fourier cross-power spectrum. Because this algorithm only



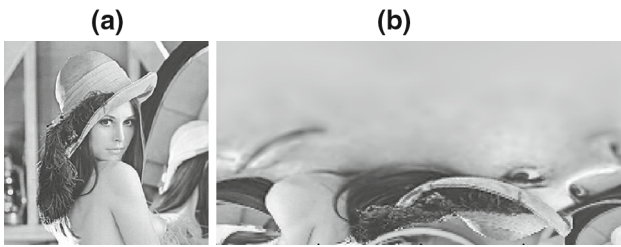


Fig. 1 Log-polar expansion of lena. *Left image* (256×256) is the original image, and the *right image* is the transformed one. The expansion origin is set to be the center of lena image, and radius = 128

takes into account the phase information in the frequency domain, the reliance on the spatial information is remarkably reduced, which leads to a relatively robust matching approach compared to the spatial ones.

We now describe how to implement phase correlation to detect the forgery in images. For a normalized rectangular image $N(x, y)$, which is obtained by expanding and interpolating the scanning patch in the log-polar coordinates, its discrete Fourier transform (DFT) can be represented as:

$$F(u, v) = \sum_{x=0}^{m-1} \sum_{y=0}^{n-1} N(x, y) e^{[-2\pi i(ux/m+vy/n)]} \quad (2)$$

We define DFT of the source patch and target patch as $F_{\text{source}}(u, v)$ and $F_{\text{target}}(u, v)$, respectively, and the corresponding correlation, which is called cross-power spectrum, is defined as:

$$C(u, v) = \frac{F_{\text{source}}(u, v) \times F_{\text{target}}^*(u, v)}{\|F_{\text{source}}(u, v) \times F_{\text{target}}^*(u, v)\|} \quad (3)$$

where $F^*(u, v)$ represents the complex conjugate of $F(u, v)$. In the next step, the inverse Fourier transform of C is calculated as:

$$R(x, y) = \frac{1}{mn} \sum_{u=0}^{m-1} \sum_{v=0}^{n-1} C(u, v) e^{[2\pi i(ux/m+vy/n)]} \quad (4)$$

Fourier shift theorem proves that the shift between two patches is equivalent to the phase difference in frequency domain. Thus, if there is only translation between two patches, by taking the inverse Fourier transform of the cross-power spectrum, a unit pulse function can be obtained.

$$(x_{\text{peak}}, y_{\text{peak}}) = \arg \max_{(x, y)} R(x, y) \quad (5)$$

Observing Eq. 5, we find that R will reach the peak value on $(x_{\text{peak}}, y_{\text{peak}})$, while on the other positions, values should be close to 0. In this way, we can estimate the shift according to the peak position. The peak value of the pulse function is

highly related to how much the content of patches overlaps. If two patches share the same content but only a shift, the peak value will reach 1, while on the other positions, the values are all 0. Along with the decreasing shared content, the peak value becomes lower.

For detecting forgery in an image, we partition the image into overlapping patches. Assuming the patch size is $a \times b$ and the step length is s , then for an image with size $l_{\text{height}} \times l_{\text{width}}$, the number of the overlapping patches is calculated by Eq. 6.

$$C_{\text{patch}} = \left(\left\lfloor \frac{l_{\text{height}} - a + 1}{s} \right\rfloor + 1 \right) \times \left(\left\lfloor \frac{l_{\text{width}} - b + 1}{s} \right\rfloor + 1 \right) \quad (6)$$

Since each patch is transformed to a rectangle in log-polar coordinates, its shape in the original coordinates should be a disk; hence, $a = b$. From the above equation, we can see that the number of patches is inversely proportional to s^2 , which means that with the increasing step size, the searching space can be significantly reduced. However, a big step will likely result in a poor detecting performance; therefore, a trade-off should be carefully considered. In our implementation, the step size is set to be 2, which provides an acceptable searching speed as well as detection accuracy.

2.3 Improved Adaptive Band Limitation

For natural images, the main feature frequency usually concentrates on the medium-low band. Based on this observation, the band limitation procedure is firstly proposed by [16]. We implement this procedure to recognize the fingerprint. By using the band limitation, the peak value of the inverse Fourier transform of the correlation matrix is significantly enhanced. In a following paper by [17], the correlation matrix is further normalized, resulting in a regularized range [0, 1]. The normalized band limitation is shown to be very effective in iris recognition.

In region duplication detection, the tampered region is always post-processed under manipulations such as adding noise, blurring or compression. Besides, due to the bilinear interpolation procedure introduced in Sect. 2.1, some information in high frequency is contaminated or even lost. All the aforementioned factors unfortunately lead to certain difficulties in detecting forgery by using canonical phase correlation. In this paper, we introduce a band limitation scheme to solve this problem.

See Fig. 2, our band limitation $L(\cdot)$ can be formulated as follows. Suppose that $F_{\text{source}}^{\text{center}}$ and $F_{\text{target}}^{\text{center}}$ are the discrete Fourier transform of the expanded source patch and target patch in which the 0 frequency has been shifted and centered, where $u \in 0, 1, \dots, m-1$ and $v \in 0, 1, \dots, n-1$, m and n are the height and width of the expanded patch, respectively.



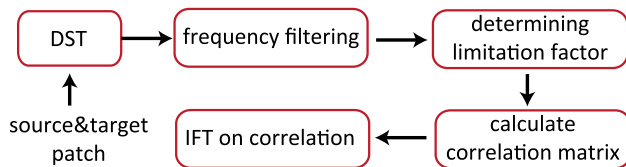


Fig. 2 Flowchart of the adaptive band limitation



Fig. 3 Example of sub-patches for estimating general fractal dimension in log-polar coordinates

Then, with the limitation factor σ , we can implement the band limitation as follows.

$$\begin{cases} L(F_{\text{source}}^{\text{center}}(u, v)) = L_{\text{source}}(u_L, v_L) \\ L(F_{\text{target}}^{\text{center}}(u, v)) = L_{\text{target}}(u_L, v_L) \end{cases} \quad (7)$$

where $u_L \in [m\sigma/2] - 1, \dots, m - [m\sigma/2] - 1$ and $v_L \in [n\sigma/2] - 1, \dots, n - [n\sigma/2] - 1$. In this step, the high-frequency part is cut off from the Fourier matrix and the rest of the band forms a new medium-low frequency matrix. Then, we calculate the correlation matrix of L_{source} and L_{target} , and implement inverse Fourier transform on the correlation, then obtain a result matrix whose peak can be remarkably enhanced.

Limitation factor σ plays an important role in the band limitation and determines how much band should be discarded, and we propose an effective method to determine σ . In the previous works [16, 17], the factor σ is specified according to different database. In [10], a piecewise linear function with respect to the local fractal dimension is proposed to control the limitation factor according to different image natures. This algorithm works very well for a polar expansion using bilinear interpolation, but when we implement the same algorithm on the log-polar coordinate, the performance degrades. This happens because conventional band limitation is presented in terms of polar expansion, in which counting a unit step length to the center point on original patch is equivalent to counting one pixel in the expanded patch; however, it is not true in the log-polar framework. In general, if a disk centered at origin in Cartesian coordinates is mapped to a rectangle with length k_1 and the circle

around the disk by stepping the same radius is mapped to a rectangle with length k_2 , then we have $k_1 > k_2$. Thus, in an understandable manner, local frequency at the point near the center is reduced, while local frequency at the point far from the center is enhanced. The proposed improved band limitation procedure is based on this observation.

In this procedure, a 32×32 patch is partitioned into four overlapping sub-patches centered at the same point with lengths 4, 8, 16 and 32, respectively. This partition is shown in Fig. 3. For ease of visualization, we choose the famous “lena” image to demonstrate the partition result. Size of these sub-patches are selected according to the log operator; thus, results will be 2, 3, 4 and 5, accordingly. Denote the four sub-patches with SP_1, \dots, SP_4 , we calculate the fractal dimension of each sub-patch using box fractal dimension estimation algorithm proposed by [18] and obtain the corresponding fractal dimension $\text{Dim}_1, \dots, \text{Dim}_4$. Next, we give a general fractal estimation Dim_g for the expanded patch as the average of $\text{Dim}_1, \dots, \text{Dim}_4$. At last, we calculate the limitation factor σ according to the value of Dim_g using the piecewise linear function proposed by [10], see Eq. 8.

$$\sigma = \begin{cases} 0.5 & \text{Dim}_g < 2.1 \\ 0.5 + 0.6(\text{Dim}_g - 2.1) & 2.1 \leq \text{Dim}_g \leq 2.6 \\ 0.8 & \text{Dim}_g > 2.6 \end{cases} \quad (8)$$

For a pair of patches to be matched, we estimate general fractal dimension of each patch and choose the smaller dimension as the limitation factor to be used in band limitation.

2.4 Strategy for Forgery Region Marking

The strategy to marking a duplicated region, which strongly influences the performance, is an important procedure in forgery detection since image proportion around the contour of forgery region is always hard to handle. In this paper, we introduce a strategy which is different from previous ones. This strategy starts from marking matched pairs of image patches on the center points. After the whole image is scanned and detected, some points which may be isolated or connected to other ones will appear in the mask image. In a sense that detected points from the same region will cluster, we can easily discard some singular or isolated points which are far from the others. Assuming that a detected point is $d_{x,y}$, we define its neighborhood corresponding to the patch radius as:

$$\text{Neighborhood}(d_{x,y}) = \{d_{u,v} | (x-u)^2 + (y-v)^2 < 16\} \quad (9)$$

Thus, if $\text{Neighborhood}(d_{x,y}) = 0$, which means that no other detected center points are inside the neighborhood of $d_{x,y}$, this point is judged to be isolated. For all the detected



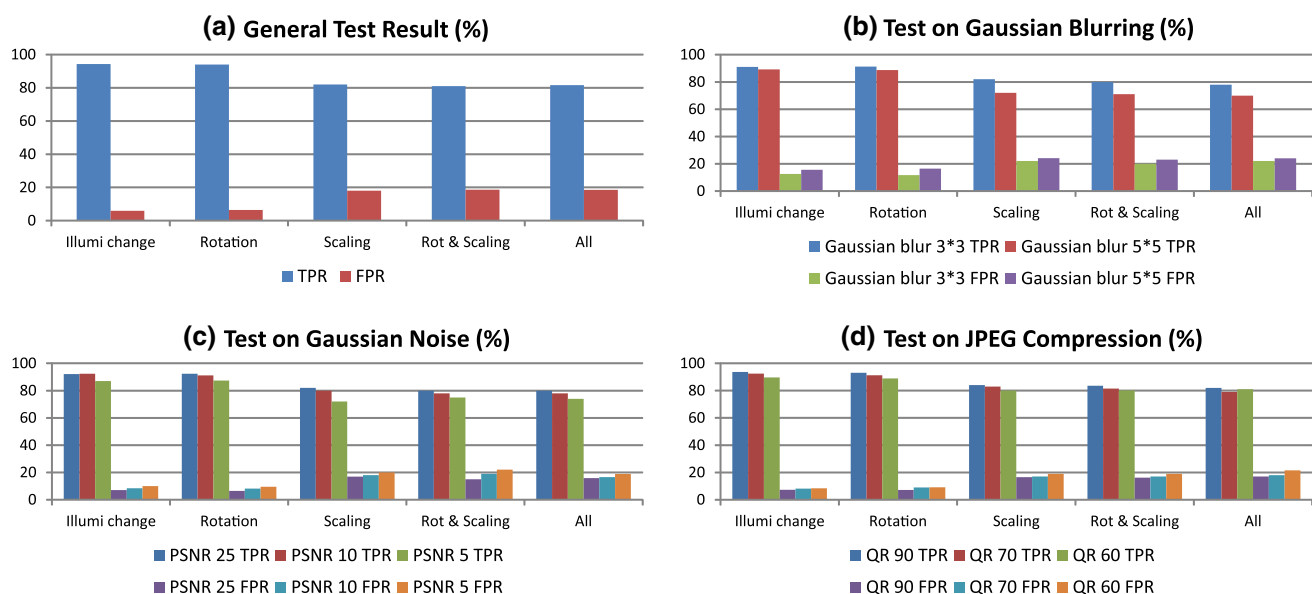


Fig. 4 Robustness test result. Illumi represents “illuminance” while QR for “quality factor” and Rot for “rotation”

center points which are not isolated points, we expand the point with a disk patch with radius 16, and points inside the disk are marked as detected subregions. At last duplicated region is marked by the union of all subregions.

3 Experiments and Analysis

In this section, we first test our algorithm on tampered images with various types of manipulations as well as degradations. The result shows the robustness and versatility of our approach. Then, comparison is made compared with other algorithms. Experimental results show the advantages of our algorithm. To evaluate the performance of the proposed algorithm, we employed a common metric (TPR(true positive rate) and FPR(false positive rate)) in region duplication detection scope, which are defined as:

$$TPR = \frac{|C \cap C'| + |M \cap M'|}{|C + M|} \quad (10)$$

$$FPR = \frac{|C - C'| + |M - M'|}{|C + M|} \quad (11)$$

where C and M represent the sum of pixels in original region and forgery region of source image, respectively, while C' and M' represent the sum of pixels in original region and forgery region of detected image, respectively.

3.1 Robustness Test and Analysis

In this part, we randomly select 50 natural images to generate 150 forgery images, including various manipulations such as

Table 1 Test cases, where Ill represents “illuminance” and Rot for “rotation”

Test case	Range	Image number
Illumination changes	Grayscale [-50, 50]	20
Rotation	Degree [0, 360]	20
Scaling	Resize [0.3, 6.0]	30
Rotation and scaling	Combinatorial	40
All	Combinatorial	40

illuminance change, rotation, scaling. The description of the benchmark is shown in Table 1, and the test result is shown in Fig. 4. It can be seen that our algorithm can detect forgery with high accuracy, while it preserves a low false detection rate. In the cases of illuminance change and rotation, TPR reaches over 90 % and FPR is below 7 %. While in the cases containing scaling, TPR decreases to around 80 % and FPR increases to around 18 %. In our test, for scaling between 0.3 and 6, the detection performance decreases, but can still give acceptable results and locate the forgery with relatively high precision.

To further verify the robustness of our algorithm against image degradations, we choose 50 test images with various manipulations, and contaminate them using various degrees of blurring, Gaussian noise, rotation and scaling. The test result is shown in Fig. 5. From the results, we can find that the performance of our algorithm drops a little when forgery consists of blur and scaling. Because the blurring will affect some part of the medium-low frequency band. However, our algorithm can still find sufficient information by using adaptive band limitation, leading to acceptable detection result. In the



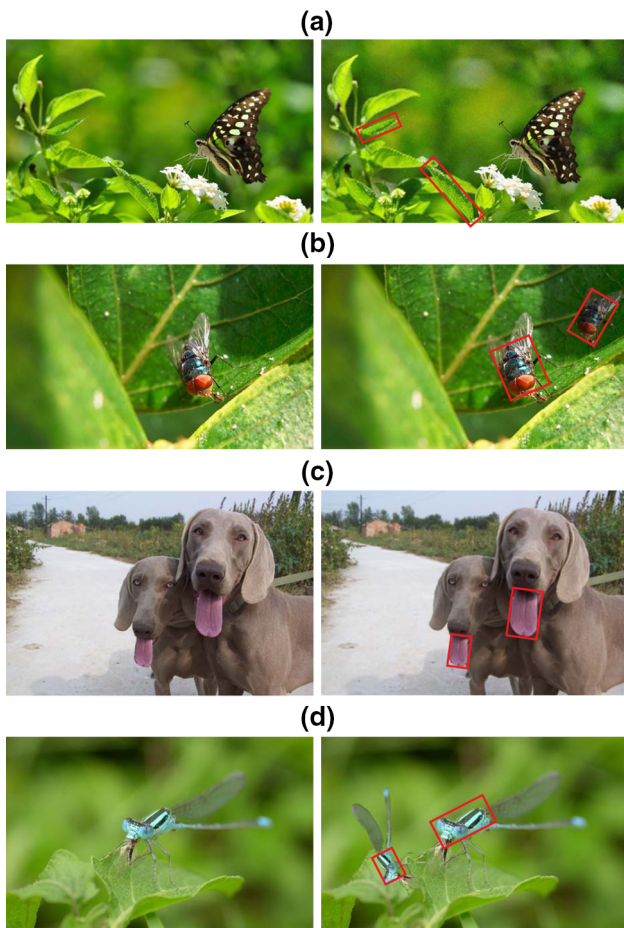


Fig. 5 Degradation test results. **a** Original image, detection result with Gaussian noise; **b** original image, detection result with quality factor 60 & scaling & rotation; **c** original image, detection result with 5*5 blur & scaling; **d** original image, detection result with quality factor 40 & scaling rotation

case of Gaussian noise and JPEG compression, our algorithm maintains stability and reliability. Experimental results show that large scaling affects detection performance more than other manipulations or degradations, which demonstrates the robustness of our algorithm to difficult situations.

3.2 Comparison Test and Analysis

We compare our algorithm with several approaches proposed by [6, 7, 10]. The test is implemented in terms of various manipulations and several levels of degradations, see Fig. 6. We only present TPR here because it has already been provided to be effective under the performance evaluation. It is easy to see that our algorithm achieved almost the same detection performance as the one proposed by [7] in general test without degradations, while other two algorithms do not perform well under scaling. However, when the images are contaminated by Gaussian noise, the stability of [7] declines

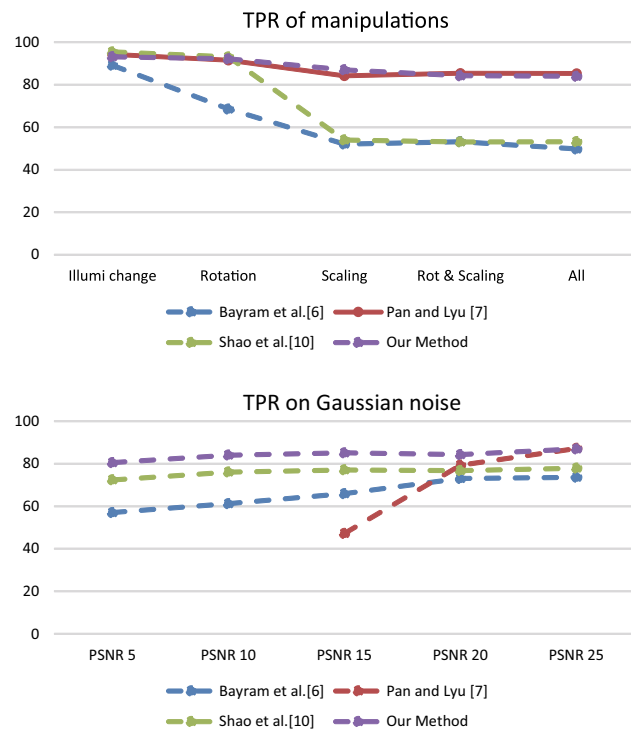


Fig. 6 Manipulations and degradations of different algorithms test result. PSNR represents “peak signal-to-noise ratio”

sharply along with the noise level. The other two algorithms always suffer from manipulation of scaling.

To further evaluate the effectiveness of our method, we detect the duplicated objects in tampered images on public dataset MICC-F220, which is composed of 220 images (110 are tampered and 110 originals). Figure 7 shows four groups of detection results, which consist of scaling and rotation. Table 2 shows FPR, TPR, processing of [19] and our method, which shows the advantages of our method.

It is supported by our test that our algorithm is relatively more effective for detecting large scaling forgery in images. In particular, based on the work by [10], the proposed algorithm maintains the strong robustness and reliability for detecting rotation. Moreover, despite to severe degradations, the proposed improved adaptive band limitation procedure generally works with higher accuracy and robustness than the ones in comparison.

4 Conclusion

In this paper, we present a robust image forgery detection approach, which works under framework of log-polar expansion and phase correlation. With improved adaptive band limitation, the proposed algorithm can locate intrinsic feature band of an image patch in frequency domain and detect duplicated regions with significant reliability and robustness. We



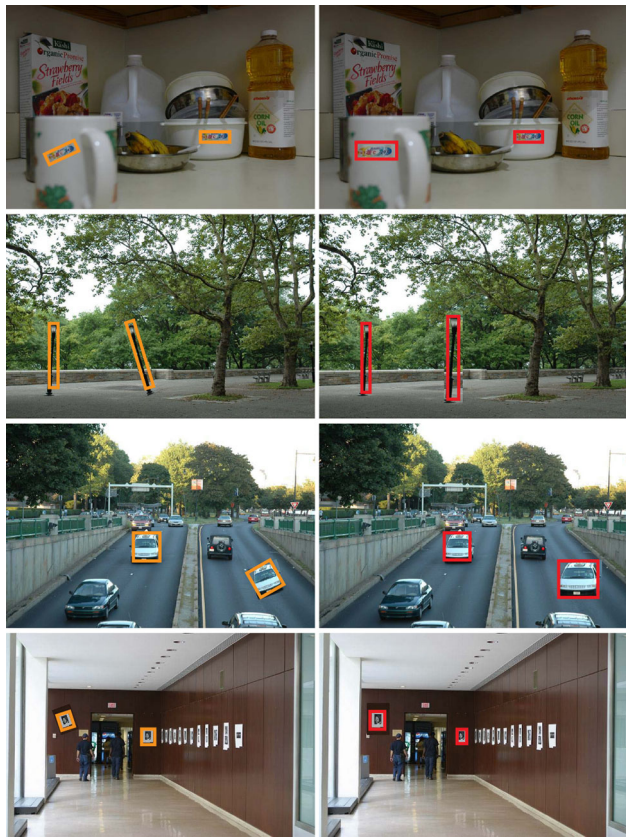


Fig. 7 Duplicated objects detection in tampered images (*Left*: rotation; *Right*: scaling) on public dataset

Table 2 FPR, TPR and processing time (average time per image) of [19] and our method

Method	FPR (%)	TPR (%)	Time (s)
Amerini et al. [19]	8	95	6.54
Our method	6	99	4.72

test our algorithm on various datasets including manipulations and degradations. Experiments show that our algorithm has remarkable performance on detecting forgery with large scaling.

Acknowledgements We thank all anonymous reviewers for their valuable comments. This research was supported by Zhejiang Provincial Natural Science Foundation of China under Grant No. LY14F020050.

References

1. Fridrich, J.; Soukal, D.; Lukas, J.: Detection of copy-move forgery in digital images. In: Proceedings of Digital Forensic Research Workshop (2003)
2. Popescu, A.C.; Farid, H.: Exposing digital forgeries by detecting duplicated image regions. Technical Report, Dartmouth College, Computer Science (2004)
3. Li, G.; Wu, Q.; Tu, D.; Sun, S.: A sorted neighborhood approach for detecting duplicated regions in image forgeries based on dwt and svd. In: Multimedia and Expo, 2007 IEEE International Conference on. pp. 1750–1753 (2007)
4. Gul, G.; Avcibas, I.; Kurugollu, F.: SVD based image manipulation detection. In: Proceedings of the International Conference on Image Processing, ICIP 2010. September 26–29, Hong Kong, China, pp. 1765–1768 (2010)
5. Mahdian, B.; Saic, S.: Detection of copy-move forgery using a method based on blur moment invariants. *Forensic Sci. Int.* **171**(2–3), 180–189 (2007)
6. Bayram, S.; Senear, H.T.; Memon, N.D.: An efficient and robust method for detecting copy-move forgery. In: Proceedings of the IEEE International Conference on Acoustics, Speech, and Signal Processing, ICASSP 2009. 19–24 April 2009, Taipei, Taiwan, pp. 1053–1056 (2009)
7. Pan, X.; Lyu, S.: Region duplication detection using image feature matching. *IEEE Trans. Inf. Forensics Secur.* **5**(4), 857–867 (2010)
8. Ryu, S.; Lee, M.; Lee, H.: Detection of copy-rotate-move forgery using zernike moments. In: Information Hiding—12th International Conference, IH 201. Calgary, AB, Canada, June 28–30, 2010, Revised Selected Papers, pp. 51–65 (2010)
9. Bravo-Solorio, S.; Nandi, A.K.: Automated detection and localisation of duplicated regions affected by reflection, rotation and scaling in image forensics. *Sig. Process.* **91**(8), 1759–1770 (2011)
10. Shao, H.; Yu, T.; Xu, M.; Cui, W.: Image region duplication detection based on circular window expansion and phase correlation. *Forensic Sci. Int.* **222**(1–3), 71–82 (2012)
11. Wang, T.; Tang, J.; Luo, B.: Blind detection of region duplication forgery by merging blur and affine moment invariants. In: Proceedings of the Seventh International Conference on Image and Graphics, ICIG 2013. Qingdao, China, July 26–28, 2013, pp. 258–264 (2013)
12. Chen, L.; Lu, W.; Ni, J.; Sun, W.; Huang, J.: Region duplication detection based on harris corner points and step sector statistics. *J. Vis. Commun. Image Represent.* **24**(3), 244–254 (2013)
13. Kuo, T.; Lo, Y.; Huang, S.: Image forgery detection for region duplication tampering. In: Proceedings of the 2013 IEEE International Conference on Multimedia and Expo, ICME 2013. San Jose, CA, USA, July 15–19, pp. 1–6 (2013)
14. Zheng, J.; Chang, L.: Detection of region-duplication forgery in image based on key points binary descriptors. *J. Inf. Comput. Sci.* **11**(11), 3959–3966 (2014)
15. Tan, M.; Hu, Z.; Wang, B.; Zhao, J.; Wang, Y.: Robust object recognition via weakly supervised metric and template learning. *Neurocomputing* **181**, 96–107 (2016)
16. Ito, K.; Nakajima, H.; Kobayashi, K.; Aoki, T.; Higuchi, T.: A fingerprint matching algorithm using phase-only correlation. *IEICE Trans. Fundam. Electron. Commun. Comput. Sci.* **97**(3), 682–691 (2004)
17. Miyazawa, K.; Ito, K.; Aoki, T.; Kobayashi, K.; Nakajima, H.: An effective approach for iris recognition using phase-based image matching. *IEEE Trans. Pattern Anal. Mach. Intell.* **30**(10), 1741–1756 (2008)
18. Sarkar, N.; Chaudhuri, B.: An efficient differential box-counting approach to compute fractal dimension of image. *IEEE Trans. Syst. Man Cybern.* **24**(1), 115–120 (1994)
19. Amerini, I.; Ballan, L.; Caldelli, R.; Bimbo, A.D.; Serra, G.: A sift-based forensic method for copy-move attack detection and transformation recovery. *IEEE Trans. Inf. Forensics Secur.* **6**(3–2), 1099–1110 (2011)

